Observation of ultraslow stress release in silicon nitride films on CaF2

Tianyi Guo, M. Jamal Deen, Changqing Xu, Qiyin Fang, P. Ravi Selvaganapathy, and Haiying Zhang

Articles you may be interested in

Dual mechanical behaviour of hydrogen in stressed silicon nitride thin films
J. Appl. Phys. **116**, 043506 (2014); 10.1063/1.4887814

Modeling stress development and hydrogen diffusion in plasma enhanced chemical vapor deposition silicon nitride films submitted to thermal cycles
J. Appl. Phys. **114**, 154113 (2013); 10.1063/1.4826208

Methods of producing plasma enhanced chemical vapor deposition silicon nitride thin films with high compressive and tensile stress
J. Vac. Sci. Technol. A **26**, 517 (2008); 10.1116/1.2906259

Stress development kinetics in plasma-enhanced chemical-vapor-deposited silicon nitride films
J. Appl. Phys. **97**, 114914 (2005); 10.1063/1.1927708

Analysis of stress and composition of silicon nitride thin films deposited by electron cyclotron resonance plasma-enhanced chemical vapor deposition for microfabrication processes
J. Vac. Sci. Technol. B **23**, 168 (2005); 10.1116/1.1835316

Observation of ultraslow stress release in silicon nitride films on CaF$_2$

Tianyi Guo
School of Biomedical Engineering, McMaster University, 1280 Main St W, Hamilton, Ontario L8S 4K1, Canada and Institute of Microelectronics, Chinese Academy of Science, Beijing 100029, China

M. Jamal Deen[a)]
Department of Electrical and Computer Engineering, McMaster University, 1280 Main St W, Hamilton, Ontario L8S 4K1, Canada and School of Biomedical Engineering, McMaster University, 1280 Main St W, Hamilton, Ontario L8S 4K1, Canada

Changqing Xu and Qiyin Fang
Department of Engineering Physics, McMaster University, 1280 Main St W, Hamilton, Ontario L8S 4L7, Canada

P. Ravi Selvaganapathy
Department of Mechanical Engineering, McMaster University, 1280 Main St W, Hamilton, Ontario L8S 4L7, Canada

Haiying Zhang
Institute of Microelectronics, Chinese Academy of Science, Beijing 100029, China

Silicon nitride thin films are deposited by plasma-enhanced chemical vapor deposition on (100) and (111) CaF$_2$ crystalline substrates. Delaminated wavy buckles formed during the release of internal compressive stress in the films and the stress releasing processes are observed macroscopically and microscopically. The stress release patterns start from the substrate edges and propagate to the center along defined directions aligned with the crystallographic orientations of the substrate. The stress releasing velocity of SiN$_x$ film on (111) CaF$_2$ is larger than that of SiN$_x$ film with the same thickness on (100) CaF$_2$. The velocities of SiN$_x$ film on both (100) and (111) CaF$_2$ increase with the film thickness. The stress releasing process is initiated when the films are exposed to atmosphere, but it is not a chemical change from x-ray photoelectron spectroscopy. © *2015 American Vacuum Society.* [http://dx.doi.org/10.1116/1.4923029]

I. INTRODUCTION

Thin films coated onto substrates by sputtering or vapor deposition often suffer from high residual stress, either compressive or tensile, which usually causes film buckling or cracking. In most cases, biaxial compressive stresses exist in the film, one of which causes the buckling with finite width and height, while the other perpendicular stress cause the buckling propagation in a sinusoidal manner, called the telephone cord mode.[1] These buckling morphologies formed in thin films to release internal compressive stresses were observed in many film/substrate combinations, including carbon/quartz glass and carbon/Si,[1–7] boron/glass,[2] TiC/quartz,[8] permalloy/Si and permalloy/glass,[9] bcc stainless steel/fcc stainless steel,[10] and aluminum/glass.[11] The buckling was generally considered as a film failure and undesirable, but its profile can be used to determine the mechanical properties of the film, such as Young's modulus,[2–5,8] because the buckling formation requires appropriate combination of the internal film stress and interface adhesion force; otherwise, the film will either adhere to or fully delaminate from the substrate. Note all these film/substrate systems[1–11] were stiff films on rigid substrate.

Recently, many researchers focused on the stiff films on compliant substrates, for example, gold film on polydimethylsiloxane, because they can form ordered structures spontaneously[12–14] and some novel applications, such as phase grating, nanochannels for protein concentration, or smart adhesion.[15–17] The films capitalize on the large elastic modulus mismatch between the film and substrate to obtain wrinkling of the substrate surface and consequently wrinkling of the stiff film. However, in stiff films on rigid substrate, ordered patterns forming spontaneously have not been reported before, although the formation of wavy buckling can be controlled by artificially introducing low adhesion area on the substrate by lithographically patterning[1] or laser beam scanning.[11]

A new film/substrate combination, silicon nitride (SiN$_x$)/calcium fluoride (CaF$_2$), is investigated to further reveal the influence of the rigid substrate on the formation of the telephone cord buckles. In addition, the study on the film instability of SiN$_x$ on CaF$_2$ will be beneficial for fabrication of novel CaF$_2$ based devices. CaF$_2$ has an optical transmission range of 150–9000 nm, from ultraviolet to middle infrared. Together with its insolubility in water, it is a promising material to make devices allowing simultaneous spectral analyses of aqueous samples in multiple regions, for example, quantitative determination of cell concentration in the visible range and qualitative identification by IR spectroscopy.[18–21] These applications requires CaF$_2$ based devices with microstructures, such as microfluidic channels for fluid handling or micropillar arrays for dielectrophoretic concentrating microbes in

a)Electronic mail: jamal@mcmaster.ca

water,[22–24] which asks for dielectric thin films that act as protective layer or etching mask. For this application, SiN_x film is a good choice as it has been widely used in micro-optoelectromechanical systems and microelectromechanical systems. Therefore, SiN_x thin films are coated onto CaF_2 substrates by plasma-enhanced chemical vapor deposition (PECVD) and the buckling formation processes are studied.

II. EXPERIMENT

CaF_2 crystal substrates of (100) and (111) orientations and area $10 \times 10 \, mm^2$, 1.0 mm-thick, and surface roughness of less than 2.5 nm were purchased from MTI Corporation. SiN_x films with thicknesses in the range of 50–200 nm were deposited on (100) and (111) CaF_2 substrates by PECVD at 300 °C with a deposition rate of 8.33 nm/min by the following reaction:

$$3SiH_4(g) + 4NH_3(g) \xrightarrow[T]{RF} Si_3N_4(s) + 12H_2(g).$$
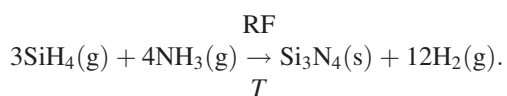
The reactant gas flow rates were 7.15 standard cubic centimeters per minute (sccm) for silane (SiH_4) and 900 sccm for ammonium (NH_3). The chamber pressure was stabilized to 87 Pa during the reaction and 50 W power of a 13.56 MHz radio frequency source used to ionize the reactant gas molecules.

III. RESULTS AND DISCUSSION

Immediately after removing the CaF_2 substrates with 100 nm SiN_x films from the PECVD chamber, they were observed under a microscope, as shown in Fig. 1: (a) and (b) for SiN_x on (100) CaF_2 and (c) and (d) for (111) CaF_2. Note that Figs. 1(b) and 1(d) are magnified view of the regions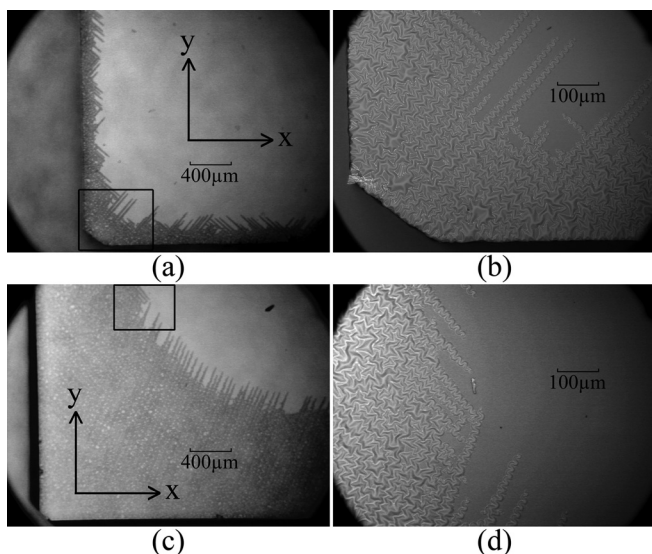 indicated by the rectangles in (a) and (c), respectively. Wrinkles formed initially at the edges of both (100) and (111) CaF_2 substrates and telephone cord buckles propagated along defined directions in the inner periphery of the wrinkled area. These views show that the stress releasing process is initiated from the substrate edges where the periodical crystalline structure of CaF_2 ends and it develops along defined orientations of CaF_2 substrate, not randomly.

The crystal orientations of the horizontal and vertical edges (x and y directions in Fig. 1) of (100) CaF_2 are $[01\bar{1}]$ and $[011]$, respectively, but are $[\bar{1}10]$ and $[\bar{1}\bar{1}2]$ for (111) CaF_2. On the (100) CaF_2 substrate, the two orientations along which the telephone cord buckles propagate are at $\pm 45°$ angle with respect to x axis, indicating that the buckles propagate at orientations of [010] and [001]. Angles of $\pm 60°$ show that the buckles propagate at orientations of $[\bar{1}01]$ and $[01\bar{1}]$ on the (111) CaF_2 substrate. These buckle propagating directions indicates that the in-plane stresses of SiN_x film on (100) CaF_2 are along [001] and [010] orientations and that for (111) CaF_2 are along $[\bar{1}10]$, $[12\bar{1}]$, and $[2\bar{1}\bar{1}]$ orientations, which means the film stress is related to the crystalline structure of the substrate although the film is not grown epitaxially because PECVD SiN_x films were mostly amorphous or polycrystalline at low deposition temperatures.[25]

The morphology of deposited SiN_x films on CaF_2 is studied by using x-ray diffraction analysis with the x-ray wavelength of 1.54056 Å, as shown in Fig. 2. Four peaks appear at 2θ of 25.56°, 28.26°, 32.78°, and 68.68°. According to the Bragg diffraction condition and the lattice constant of CaF_2 (5.462 Å), the latter three peaks correspond to (111), (200), and (400) CaF_2, respectively. In addition, the peak 2θ corresponding to (100) CaF_2 is calculated to be 16.21° and that for (110) CaF_2 be 23.01°, both of which are far away from 25.56°. Therefore, the peak at 25.56° can only arise from SiN_x, indicating the SiN_x films are polycrystalline.

Regarding physical origins of the stress generated in the SiN_x films, two generic mechanisms had been proposed

FIG. 1. (a) Microscopic views of 100 nm-thick SiN_x film deposited by PECVD on (100) CaF_2 [(a) and (b)] and (111) CaF_2 [(c) and (d)]. Photos were taken immediately after removing the CaF_2 substrates from the PECVD chamber. (b) and (d) are magnified views of the regions indicated by the rectangles in (a) and (c), respectively.
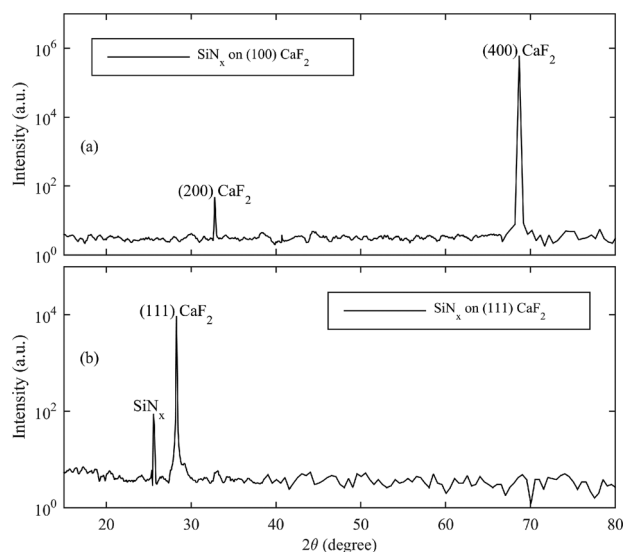

FIG. 2. XRD spectra of silicon nitride films on (100) CaF_2 (a) and (111) CaF_2 (b).

before: (1) surface stress mechanism[26–28] and (2) flux-driven incorporation of excess atoms in grain boundaries.[28,29] We prefer to recall the former because it involves the contribution from substrate. For the 100 nm SiN$_x$ films on CaF$_2$ substrate, the stress can be evaluated by the following equation:[28]

$$\sigma(h) = \sigma_0 - (f_1 + f_2)\left(\frac{1}{h_{cont}} - \frac{1}{h}\right),$$

where $\sigma(h)$ is the stress of film with thickness of h, σ_0 is the net tensile stress when the film has just become fully continuous, f_1 is the surface stress associated with the free surface of the SiN$_x$ film, i.e., the top surface, and f_2 is the interfacial surface stress associated the SiN$_x$/CaF$_2$ interface. In this model, f_1 and f_2 were assumed to be isotropic surface stresses for the simplicity of analysis. However, it is not the case for the SiN$_x$/CaF$_2$, where at least f_2 has relationship to the crystallographic structure of the CaF$_2$ substrate, which results in the stresses along [001] and [010] orientations for SiN$_x$/(100) CaF$_2$ and stresses along [$\bar{1}$10], [$\bar{1}$2$\bar{1}$], and [2$\bar{1}$$\bar{1}$] orientations for SiN$_x$/(111) CaF$_2$, and thus, the buckle propagating directions aligned with the crystallographic orientations of the CaF$_2$ substrate.

The front-end of a telephone cord buckle in Fig. 1(b) was profiled by using atomic force microscopy (AFM), shown in Fig. 3(a), which shows the buckling height of about 800 nm. Because the thickness of the SiN$_x$ film is 100 nm, much less than the buckling height, we believe the buckled film is detached from the substrate. The formation of buckles during stress releasing implies that SiN$_x$ films are compressively stressed on CaF$_2$ crystals. Figure 3(b) shows the dimensions of the buckling width, $2b = 18\ \mu$m, and the undulating wavelength, $l = 17.3\ \mu$m, of the telephone cord buckle, yielding a

$l/2b$ of 0.961, which is in agreement with previous calculations in Ref. 1. The half-width, b_0, associated with the onset of buckling is calculated to be 1.2 μm and the stress is estimated to be 1 GPa using the model in Ref. 1 with Young's modulus of 150 GPa and Poisson's ratio of 0.3 for the SiN$_x$ film.[30]

The stress releasing processes of 100 nm SiN$_x$ films on both (100) and (111) CaF$_2$ substrates were observed by recording 30 min videos under a microscope, in which four frames at the time of 0, 10, 20, and 30 min are shown in Fig. 4: (a)–(d) for (100) CaF$_2$, (e)–(h) for (111) CaF$_2$, and (a) and (e) for the time right after removing CaF$_2$ crystals from the PECVD chamber, (b) and (f), (c) and (g), and (d) and (h) for 10, 20, and 30 min
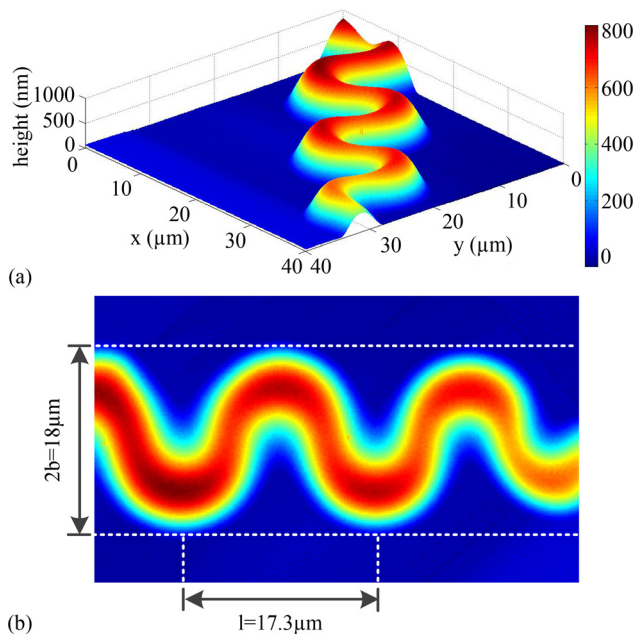

FIG. 3. (Color online) (a) Three-dimension profiling of the front-end of a telephone cord buckle by AFM; (b) measurements of the buckling width, $2b = 18\ \mu$m, and the undulating wavelength, $l = 17.3\ \mu$m.
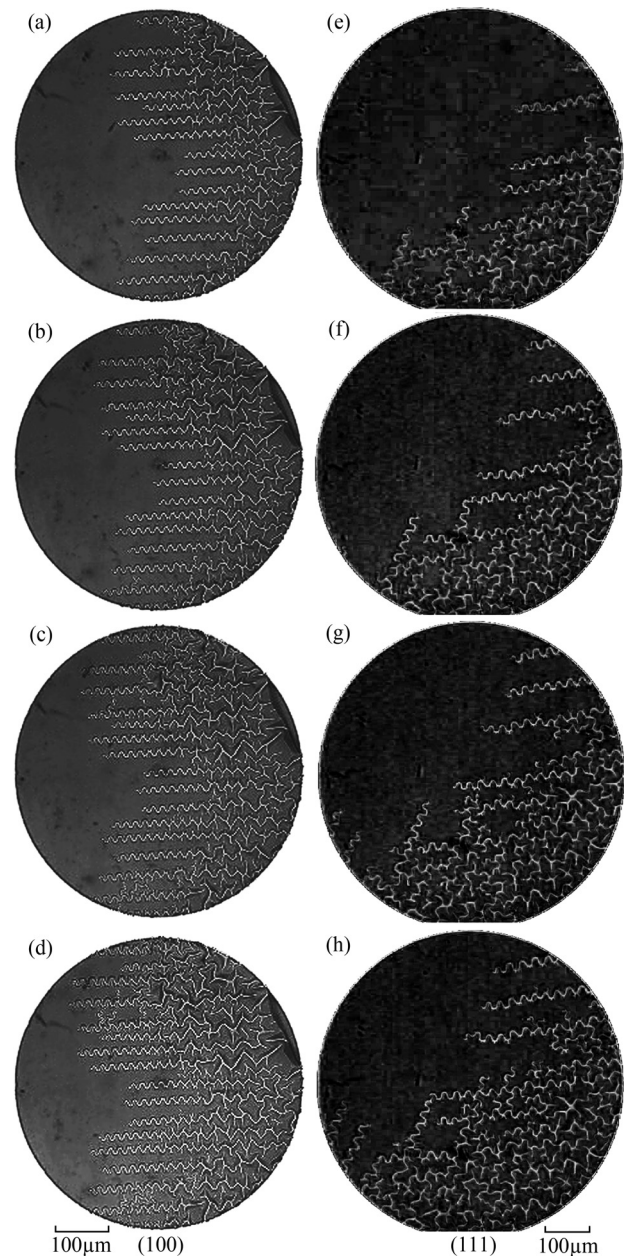

FIG. 4. Growth of the telephone cord buckles during the stress releasing processes of 100 nm SiN$_x$ films deposited by PECVD on (100) CaF$_2$ [(a)–(d)] and (111) CaF$_2$ [(e)–(h)]. [(a) and (e)]: time = 0; [(b) and (f)]: time = 10 min; [(c) and (g)]: time = 20 min; and [(d) and (h)]: time = 30 min.
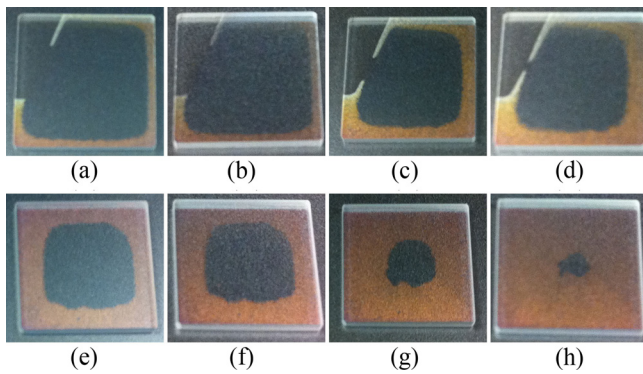
FIG. 5. (Color online) Photos of 100 nm-thick SiN_x films deposited on (100) [(a)–(d)] and (111) [(e)–(h)] CaF₂ substrates by PECVD at different time after removing them from the PECVD chamber. [(a) and (e)] time = 0; [(b) and (f)] time = 1.5 h; [(c) and (g)] time = 28 h; and [(d) and (h)] time = 67 h.
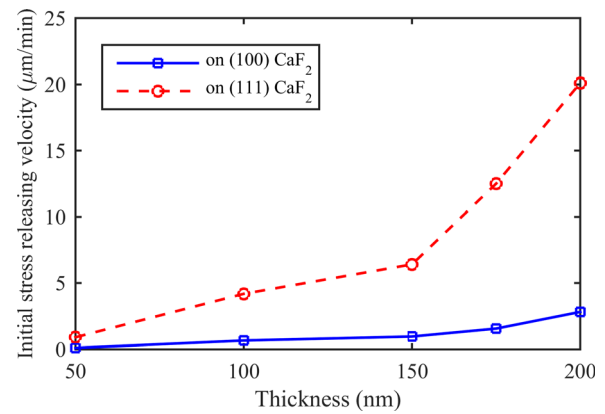

FIG. 6. (Color online) Dependence of initial stress releasing velocity of SiN_x film on (100) CaF₂ (square symbol) and (111) CaF₂ (circle symbol) on film thickness.

afterward, respectively. We can see that the telephone cord buckles are growing along certain orientations described above.

The complete processes of stress releasing were recorded macroscopically by taking photos of 100 nm SiN_x films on both (100) and (111) CaF₂ substrates at different times, as shown in Fig. 5: (a)–(d) for (100) CaF₂ and (e)–(h) for (111) CaF₂, (a) and (e) for the time right after removing both CaF₂ substrates from the PECVD chamber, (b) and (f), (c) and (g), and (d) and (h) for 1.5, 28, and 67 h afterward, respectively. The upper left corner of (100) CaF₂ crystal was covered by a silicon wafer during the deposition of SiN_x in the PECVD chamber, resulting in no SiN_x on the corner. Stress releasing indicated by the wrinkled areas starts from the substrate edges except for the corner, further proving that stress releasing is initiated from the discontinuity of the periodical crystalline structure of the substrates.

In addition, the growth of the telephone cord buckles of SiN_x on (111) CaF₂ is faster than on (100) CaF₂, perhaps due to the larger interfacial surface stress (f_2), for SiN_x/(111) CaF₂, resulting in larger internal compressive stress on (111) CaF₂. And the growing velocity decays with time for SiN_x on both (100) and (111) CaF₂. The initial stress releasing velocity of SiN_x was defined by the average propagation velocity in the first 30 min after removing SiN_x on CaF₂ from the PECVD chamber and was measured by the recorded video for different thicknesses of SiN_x, 50–200 nm, shown in Fig. 6. For the same thickness of SiN_x film, the stress releasing on (111) CaF₂ is faster than on (100) CaF₂ because the film on (111) CaF₂ exhibits a larger stress that drives the growth of buckles. Their initial stress releasing velocities increase with the film thickness, because thicker SiN_x film provides larger stress to drive the buckles growing faster.

The buckling of SiN_x films starts immediately when they were removed from the vacuum chamber and exposed to the atmosphere for films kept in vacuum for different time periods. There exists the possibility that air reacts with the film and the change of atomic ratio of SiN_x initializes the formation and growth of buckles. To investigate this possibility, the stressed and stress-released films were characterized by x-ray photoelectron spectroscopy (XPS) performed on a 100 nm-thick SiN_x film on (100) CaF₂ crystal. Using a
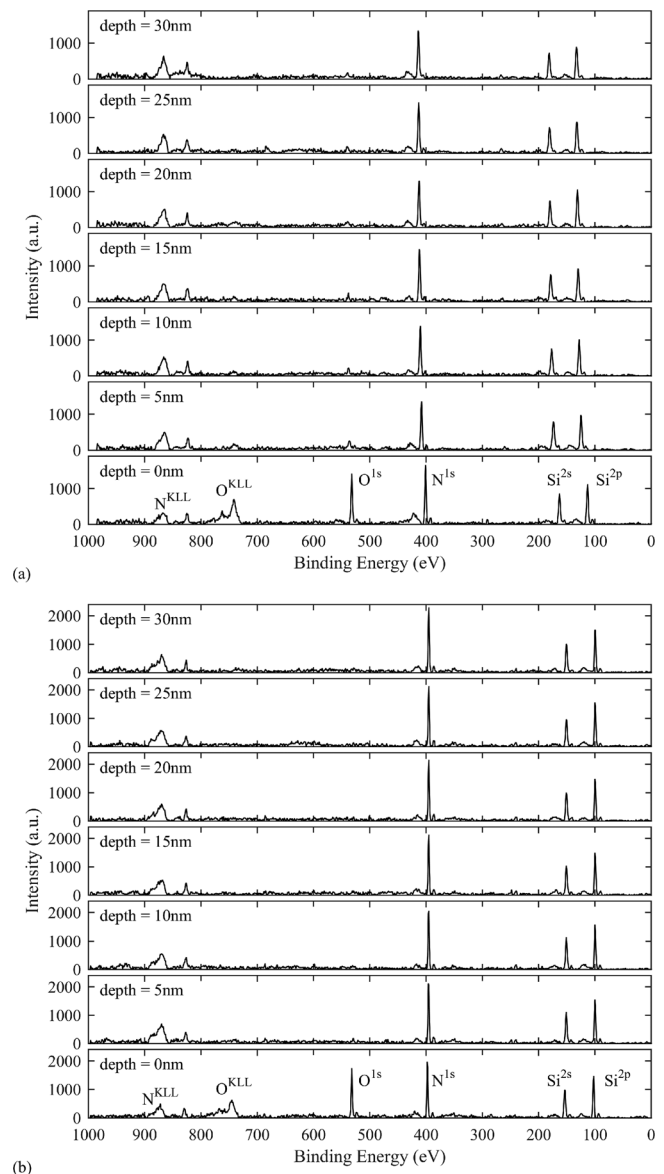

FIG. 7. Depth profile of XPS spectra of 100 nm silicon nitride film on (100) CaF₂ by PECVD. (a) Stressed area in the center of CaF₂ crystal and (b) stress-released area near the edge of CaF₂ crystal.

TABLE I. Atomic ratio of stress SiN$_x$, x_1, and stress-released SiN$_x$, x_2, calculated based on XPS analysis at different depth, d, from the surface, and their mean values, μ, and standard deviation, σ.

d (nm)	x_1	x_2
5	0.664	0.694
10	0.670	0.757
15	0.734	0.656
20	0.688	0.682
25	0.692	0.646
30	0.697	0.753
μ	0.691	0.698
σ	0.025	0.047

focused argon ion beam etching, XPS spectra of stressed SiN$_x$ in the center of CaF$_2$ [Fig. 7(a)] and stress-released SiN$_x$ near the edges of CaF$_2$ [Fig. 7(b)] were obtained at different depths from the film's top surface. In the spectra for the film's top surface, peaks corresponding to oxygen are found because of the natural oxidization of SiN$_x$ by the oxygen in air. But they disappear in the following spectra after the argon ion beam etching, indicating no oxygen exists inside SiN$_x$ films. Therefore, the spectra, except for the top surface spectrum, can be used to determine the atomic ratio of nitrogen and silicon, that is, x in SiN$_x$.

The x-ray photoelectron counts of the peaks of N and Si atoms in the spectra except for the top surface spectrum are summarized in Table I. The atomic ratio, x, of SiN$_x$ film of stressed SiN$_x$ and stress-released SiN$_x$ are 0.691 ± 0.025 and 0.698 ± 0.047, respectively. The small difference of x between stressed and stress-released SiN$_x$ demonstrates that the stress release process is a complete physical change, not a chemical change involving reaction with air.

IV. SUMMARY AND CONCLUSIONS

Silicon nitride films of a thickness of 50–200 nm are deposited by PECVD on bare (100) and (111) CaF$_2$ crystal substrates. Delaminated wavy buckles formed in the films immediately after removing the deposited CaF$_2$ crystals from the PECVD chamber are due to releasing of internal compressive stress in the films. The stress releasing processes are observed macroscopically and microscopically. Stress releasing patterns start from the substrate edges and then propagate to the centers along defined directions aligned with the crystallographic orientations of the CaF$_2$ substrate. The stress releasing velocity of SiN$_x$ film on (111) CaF$_2$ is larger than that of SiN$_x$ film with the same thickness on (100) CaF$_2$, perhaps due to the larger interfacial surface stress for SiN$_x$/(111) CaF$_2$. The velocities of SiN$_x$ film on both (100) and (111) CaF$_2$ increase with the film thickness increasing because thicker films exhibit larger stresses. Finally, the atomic ratio, x, of stress SiN$_x$ and stress-release

SiN$_x$ is analyzed by using x-ray photoelectron spectroscopy. The results show the same x, proving that the stress releasing process is a physical change.

[1]M. W. Moon, K. R. Lee, K. H. Oh, and J. W. Hutchinson, Acta Mater. **52**, 3151 (2004).
[2]A. Kinbara, S. Baba, N. Matuda, and K. Takamisawa, Thin Solid Films **84**, 205 (1981).
[3]N. Matuda, S. Baba, and A. Kinbara, Thin Solid Films **81**, 301 (1981).
[4]D. Nir, Thin Solid Films **112**, 41 (1984).
[5]G. Gille and B. Rau, Thin Solid Films **120**, 109 (1984).
[6]A. Kinbara and S. Baba, J. Vac. Sci. Technol. A **9**, 2494 (1991).
[7]M. W. Moon, H. M. Jensen, J. W. Hutchinson, K. H. Oh, and A. G. Evans, J. Mech. Phys. Solids **50**, 2355 (2002).
[8]A. Kinbara and S. Baba, Thin Solid Films **107**, 359 (1983).
[9]C. Kim, J. Vac. Sci. Technol. A **8**, 1407 (1990).
[10]J.-P. Eymery, Scr. Metall. Mater. **28**, 633 (1993).
[11]K. Xiao, Z. S. Guan, G. J. Wang, L. Jiang, D. B. Zhu, and Y. R. Wang, Appl. Phys. Lett. **85**, 1934 (2004).
[12]N. Bowden, S. Brittain, A. G. Evans, J. W. Hutchinson, and G. M. Whitesides, Nature **393**, 146 (1998).
[13]E. P. Chan and A. J. Crosby, Soft Matter **2**, 324 (2006).
[14]J. Genzer and J. Groenewold, Soft Matter **2**, 310 (2006).
[15]C. Harrison, C. M. Stafford, W. Zhang, and A. Karim, Appl. Phys. Lett. **85**, 4016 (2004).
[16]S. Chung, J. H. Lee, M.-W. Moon, J. Han, and R. D. Kamm, Adv. Mater. **20**, 3011 (2008).
[17]E. P. Chan, E. J. Smith, R. C. Hayward, and A. J. Crosby, Adv. Mater. **20**, 711 (2008).
[18]M. Kölhed, P. Hinsmann, P. Svasek, J. Frank, B. Karlberg, and B. Lendl, Anal. Chem. **74**, 3843 (2002).
[19]M. Kölhed, P. Hinsmann, B. Lendl, and B. Karlberg, Electrophoresis **24**, 687 (2003).
[20]T. Pan, R. T. Kelly, M. C. Asplund, and A. T. Woolley, J. Chromatogr. A **1027**, 231 (2004).
[21]P. Svasek, E. Svasek, B. Lendl, and M. Vellekoop, Sens. Actuators, A **115**, 591 (2004).
[22]B. H. Lapizco-Encinas, R. V. Davalos, B. a. Simmons, E. B. Cummings, and Y. Fintschenko, J. Microbiol. Methods **62**, 317 (2005).
[23]B. H. Lapizco-Encinas, B. A. Simmons, E. B. Cummings, and Y. Fintschenko, Electrophoresis **25**, 1695 (2004).
[24]M. B. Sano, R. C. Gallo-Villanueva, B. H. Lapizco-Encinas, and R. V. Davalos, Microfluid. Nanofluid. **15**, 599 (2013).
[25]K.-C. Lin and S.-C. Lee, J. Appl. Phys. **72**, 5474 (1992).
[26]R. C. Cammarata, Prog. Surf. Sci. **46**, 1 (1994).
[27]R. C. Cammarata, T. M. Trimble, and D. J. Srolovitz, J. Mater. Res. **15**, 2468 (2000).
[28]J. A. Floro, E. Chason, R. C. Cammarata, and D. J. Srolovitz, MRS Bull. **27**, 19 (2002).
[29]E. Chason, B. W. Sheldon, L. B. Freund, J. A. Floro, and S. J. Hearne, Phys. Rev. Lett. **88**, 156103 (2002).
[30]A. A. Abdallah, D. Kozodaev, P. C. P. Bouten, J. M. J. Den Toonder, U. S. Schubert, and G. de With, Thin Solid Films **503**, 167 (2006).